RSC Advances

PAPER

View Article Online
View Journal | View Issue

Cite this: *RSC Adv.*, 2021, **11**, 25995

Novel nano-architectured carbon quantum dots (CQDs) with phosphorous acid tags as an efficient catalyst for the synthesis of multisubstituted 4*H*-pyran with indole moieties under mild conditions†

Milad Mohammadi Rasooll,[a] Mahmoud Zarei,*[a] Mohammad Ali Zolfigol,*[a] Hassan Sepehrmansourie,[a] Afsaneh Omidi,[b] Masoumeh Hasani*[b] and Yanlong Gu[c]

Received 30th March 2021
Accepted 28th June 2021

DOI: 10.1039/d1ra02515e

rsc.li/rsc-advances

In this work, a new nano-structured catalyst with phosphorus acid moieties, synthesized by the reaction of carbon quantum dots (CQDs) and phosphorus acid under refluxing EtOH. The structure and morphology of CQDs–$N(CH_2PO_3H_2)_2$ were fully characterized using various techniques such as Fourier transform infrared (FT-IR) spectroscopy, transmission electron microscopy (TEM), scanning electron microscopy (SEM), energy dispersive X-ray (EDX) spectroscopy, thermogravimetric (TG) analysis, fluorescence and X-ray diffraction (XRD) measurements. The new CQDs–$N(CH_2PO_3H_2)_2$ catalyst was successfully used for the synthesis of 2-amino-6-(2-methyl-1*H*-indol-3-yl)-4-phenyl-4*H*-pyran-3,5-dicarbonitriles by the one-pot reaction of various aromatic aldehydes, 3-(1*H*-indol-3-yl)-3-oxopropanenitrile derivatives and malononitrile in refluxing EtOH and/or ultrasonic irradiation conditions.

1. Introduction

Carbon quantum dots (CQDs) have recently attracted comprehensive research interest due to their various physicochemical properties and favorable features such as biocompatibility, distinctive optical properties and low cost.[1–6] In 2004, Xu *et al.* developed carbon quantum dots (CQDs) during the purification of single-walled carbon nanotubes *via* a preparative electrophoresis methodology.[7] Carbon quantum dots (CQDs) have been used in many interesting fields of research such as bioimaging, biosensing, catalysis, heavy metal element sensing and biomolecule/drug delivery.[8–13] Also, these nanomaterials show intense photoluminescence (PL), arising from quantum-confinement effects.[14] Materials with phosphorous acid tags have been introduced as catalysts, adsorbents, inhibitors and extractants.[15] Recently a wide variety of solid acid catalysts with phosphorous acid functional groups, such as glycoluril,[16] SBA-15,[17] a melamine-based nano catalyst,[18] metal–organic frameworks (MOFs)[19–21] and uric acid,[22] have been reported for the synthesis of organic compounds.

Organic compounds with indole scaffolds have diverse biological and pharmacological applications such as antifungal, optimal inhibitory, anticholinergic, antihypertensive, antibacterial, antiviral, cardiovascular, anticonvulsant and antiproliferative activities.[23–30] Also, several natural products and pharmaceutically important compounds which act as antitumor, anticancer, anti-inflammatory, hypoglycemic, antipyretic or analgesic reagents have indole scaffolds in their structures.[31] Additionally, 4*H*-pyran derivative structures are an important category of heterocyclic compounds due to their biological properties, such as their anticoagulant, anticancer, antioxidant, spasmolytic, diuretic and anti-anaphylactic activities (Fig. 1).[32–36] 2-Amino-4*H*-pyran derivatives have also been applied as photoactive materials, cosmetics and pigments.[37] Ultrasonic irradiation has been widely applied for the preparation of organic compounds with biological activity. On the other hand, ultrasonic irradiation as an efficient strategy for the preparation of materials in chemical synthesis has received great attention in chemical processes.[38,39] One of the major advantages of ultrasonic irradiation is the controllability of the time and energy power.

[a]*Department of Organic Chemistry, Faculty of Chemistry, Bu-Ali Sina University, Hamedan 6517838683, Iran. E-mail: mahmoud8103@yahoo.com; zolfi@basu.ac.ir; mzolfigol@yahoo.com; Fax: +988 138380709; Tel: +988 138282807*

[b]*Department of Analytical Chemistry, Faculty of Chemistry, Bu-Ali Sina University, Hamedan, Iran. E-mail: hasani@basu.ac.ir*

[c]*School of Chemistry and Chemical Engineering, Huazhong University of Science and Technology, 1037 Luoyu Road, Hongshan District, Wuhan, 430074, China. E-mail: klgyl@hust.edu.cn*

† Electronic supplementary information (ESI) available. See DOI: 10.1039/d1ra02515e

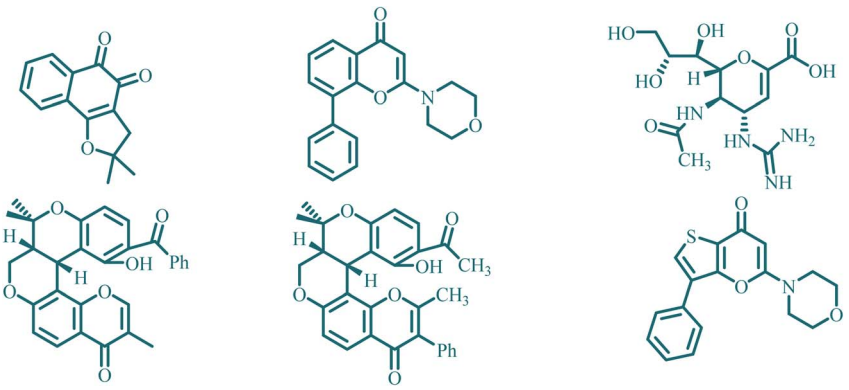

Fig. 1 Structure of pyran compounds with biological properties.

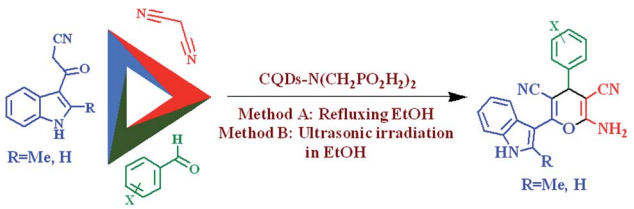

Scheme 1 Synthesis of 4*H*-pyran-3,5-dicarbonitrile with indole moieties using CQDs-$N(CH_2PO_3H_2)_2$.

On the basis of the above-mentioned facts, the synthesis of 4*H*-pyran-3,5-dicarbonitrile and pyridines with indole moieties in the presence of reusable solid acid catalysts is our main research interest. With this aim, CQDs-$N(CH_2PO_3H_2)_2$, as a novel carbon quantum dot (CQD) nano-catalyst structure with phosphorus acid tags, was synthesized, characterized and used in the synthesis of 4*H*-pyran-3,5-dicarbonitrile with indole moieties, both in refluxing EtOH and ultrasonic irradiation in EtOH as a solvent (Scheme 1).

2. Experimental

2.1. General procedure for the preparation of CQDs–$N(CH_2PO_3H_2)_2$

Initially, carbon quantum dots (CQDs) were synthesized by adding citric acid (1.05 g, 5.5 mmol), ethane-1,2-diamine (5 mmol, 0.33 mL) and 10 mL H_2O under ultrasonic irritation for 30 min.[40] Then, this mixture was kept in a Teflon-lined stainless-steel autoclave at 200 °C for 6 h. After the reaction was completed, a dark precipitate appeared, which was filtered by centrifugation (1000 rpm, 20 min). The carbon quantum dots (CQDs) were dried under vacuum. Then, in a 25 mL round-bottomed flask connected to a reflux condenser, carbon quantum dots (CQDs) (0.5 g), paraformaldehyde (4 mmol, 0.12 g), phosphorous acid (2 mmol, 0.164 g), *p*-TSA (0.01 g) and ethanol (10 mL) were added and refluxed for 8 hours. A white solid appeared, which was filtered by centrifugation (1000 rpm, 10 min). The obtained CQDs-$N(CH_2PO_3H_2)_2$ was dried under vacuum (Scheme 2).

2.2. General procedure for the synthesis of 2-amino-6-(2-methyl-1*H*-indol-3-yl)-4-phenyl-4*H*-pyran-3,5-dicarbonitrile using CQDs–$N(CH_2PO_3H_2)_2$ as a catalyst

In a 20 mL round-bottomed flask, a mixture of aldehyde (1 mmol), 3-(1*H*-indol-3-yl)-3-oxopropanenitrile derivatives (1 mmol), malononitrile (1.1 mmol, 0.073 g), CQDs–$N(CH_2PO_3H_2)_2$(10 mg) as a catalyst and EtOH (10 mL) was stirred under reflux conditions (method A) or under ultrasonic irradiation (method B). After the completion of the reaction (monitored by TLC *n*-hexane/ethyl acetate; 7 : 3), PEG (10 mL) was added to the mixture and the catalyst was separated by centrifugation (1000 rpm, 10 min). Finally, the mixture was poured into H_2O and the precipitate was filtered off. The obtained residue was washed with warm ethanol and dried at 100 °C (Scheme 1).

Scheme 2 Preparation of CQDs–$N(CH_2PO_3H_2)_2$ as the desired catalyst.

3. Result and discussion

3.1. Synthesis and characterization of the catalyst with phosphorous acid tags

Since molecules with indole moieties have been considered as candidates with biological interest[41] and we have conducted a literature survey for publishing a comprehensive review on the subject of bis and tris indolyl methanes,[42] we decided to report a catalytic methodology for the synthesis of multisubstituted 4*H*-pyran with indole moieties (Schemes 1 and 2). Here, 2-amino-6-(2-methyl-1*H*-indol-3-yl)-4-phenyl-4*H*-pyran-3,5-dicarbonitriles were successfully synthesized in the presence of CQDs–$N(CH_2PO_3H_2)_2$, various aromatic aldehydes, 3-(1*H*-indol-3-yl)-3-oxopropanenitrile derivatives and malononitrile both in refluxing EtOH and/or ultrasonic irradiation conditions.

At first, the desired catalyst CQDs–$N(CH_2PO_3H_2)_2$ was prepared according to Scheme 2. This novel nano-structure catalyst was fully characterized by applying FT-IR spectroscopy, XRD spectroscopy, FE-SEM, energy dispersive X-ray spectroscopy (EDS), transmission electron microscopy (TEM), TG and fluorescence analysis.

The FT-IR spectra of carbon quantum dots (CQDs) and CQDs–$N(CH_2PO_3H_2)_2$ are compared in Fig. 2. The broad peak at 2600–3500 cm^{-1} is related to the OH of the PO_3H_2 functional groups. The absorption bands at 1015 and 1050 cm^{-1} are related to P–O bond stretching and the band at 1128 cm^{-1} is related to P=O. The differences between the FT-IR spectra of the carbon quantum dots (CQDs) and CQDs-$N(CH_2PO_3H_2)_2$ verified the structure of the catalyst.

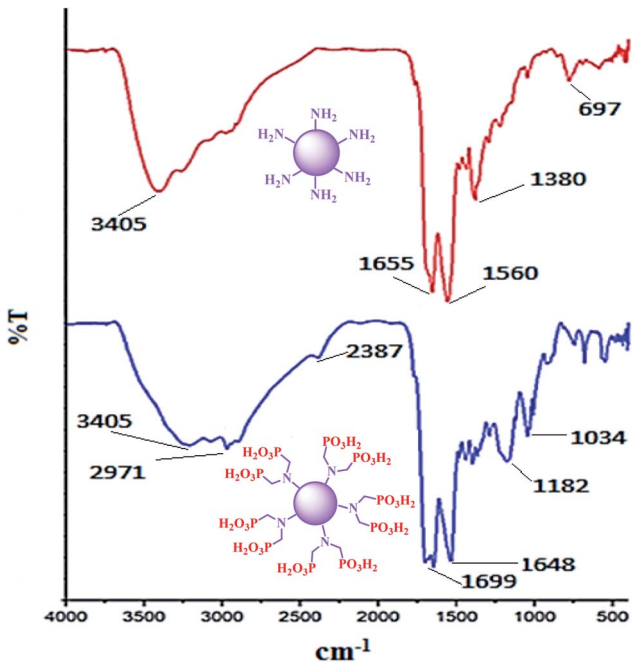

Fig. 2 Comparison of the FT-IR spectra of the CQDs and CQDs–$N(CH_2PO_3H_2)_2$.

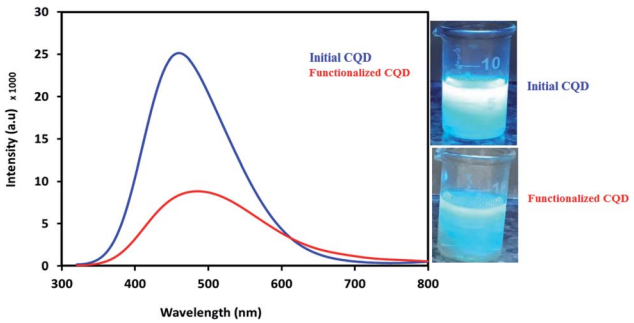

Fig. 3 Fluorescence spectra of the initial CQDs and functionalized CQDs.

Following this, the fluorescence features of the initial CQDs and functionalized CQDs were investigated for the evaluation of the synthesized CQDs and the effect of post-functionalization on the surface of the final catalyst. As can be seen in Fig. 3, the initial synthesized CQDs display a high-intensity emission peak at 450 nm (peak a). But the fluorescence intensity of the functionalized CQDs with PO_3H_2 groups is decreased and shifted towards longer wavelengths (the red shift effect). Many factors are effective for amplifying or attenuating the fluorescence intensity by affecting the resonance system, including structural rigidity, steric effect interactions, temperature, solvent, pH, the presence of para-magnetite species, heavy atoms and electron donor/acceptor groups. It can be proposed that the presence of larger PO_3H_2 groups instead of the smaller proton groups (Scheme 1) can have a negative effect on the fluorescence intensity due to the steric effects. In the other words, the presence of the large PO_3H_2 groups, along with the possible rotation of these groups, reduces the symmetry of the molecule. So, increasing the mobility of the molecule will reduce the fluorescence intensity of the functionalized CQDs due to the decreased rigidity and disturbance of the conjugated system. The decreasing fluorescence intensity of

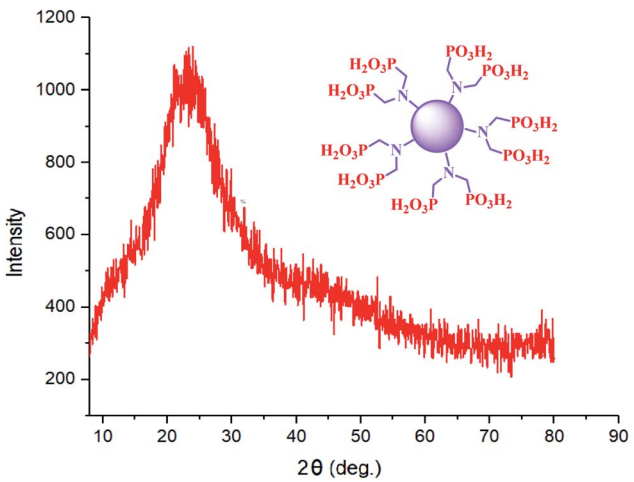

Fig. 4 X-ray diffraction (XRD) pattern of CQDs functionalized with PO_3H_2 groups.

the functionalized CQDs compared to that of the initial CQDs can be a reason for the stabilization of PO_3H_2 functional groups on the initial CQD surface. Fig. 3 shows photographic images of the decreased fluorescence intensity of the initial CQDs after post-modification with the PO_3H_2 groups.

The XRD pattern for CQDs–$N(CH_2PO_3H_2)_2$ is shown in the region of 2θ = 5–80° (Fig. 4). The broad peak of CQDs-$N(CH_2PO_3H_2)_2$ corresponds to the diffraction lines in previously reported literature.[43] Therefore, the structure and morphology of the carbon quantum dots (CQDs) is stable after functionalization with phosphorous acid groups.

The elements that CQDs–$N(CH_2PO_3H_2)_2$ was composed of were also studied with energy dispersive X-ray (EDX) analysis (Fig. 5). The structure of the catalyst was verified by the existence of N, C, O and P atoms.

The morphology and particle size of CQDs–$N(CH_2PO_3H_2)_2$ were also studied from the scanning electron microscopy (SEM) (Fig. 6a and b) and transmission electron microscopy (TEM) images (Fig. 7). The scanning electron microscopy (SEM) of CQDs–NH_2 (Fig. 6a) and CQDs–$N(CH_2PO_3H_2)_2$ (Fig. 6b) did not show different morphologies of these materials. As shown in the transmission electron microscopy images (Fig. 7), nanoparticles of CQDs-$N(CH_2PO_3H_2)_2$ are approximately 5–15 nm with a narrow size, which are regularly arranged and not completely stacked.

The thermal gravimetric (TG) analysis results for CQDs–$N(CH_2PO_3H_2)_2$ are shown in Fig. 8. Two declining stages were observed for CQDs–$N(CH_2PO_3H_2)_2$ in Fig. 8. The first weight loss (which includes about 5% weight loss) was related to the evaporation of the solvents (organic and water). The second weight loss is at 400 °C (includes about 40% weight loss), which is linked to the breaking of the bonds of N–C–PO_3H_2 of the structure of CQDs–$N(CH_2PO_3H_2)_2$.

3.2. Catalytic properties of the catalyst with phosphorous acid tags

After the synthesis and characterization of CQDs–$N(CH_2PO_3H_2)_2$, it was applied for the synthesis of 2-amino-6-(2-methyl-1*H*-indol-3-yl)-4-phenyl-4*H*-pyran-3,5-dicarbonitrile derivatives with indole and pyran moieties. The above-mentioned products were obtained by the

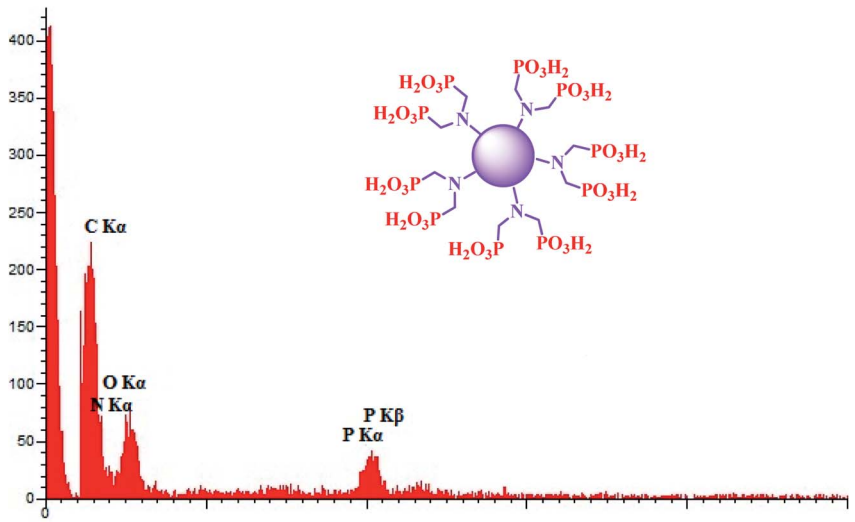

Fig. 5 Energy dispersive X-ray (EDX) analysis of CQDs–$N(CH_2PO_3H_2)_2$.

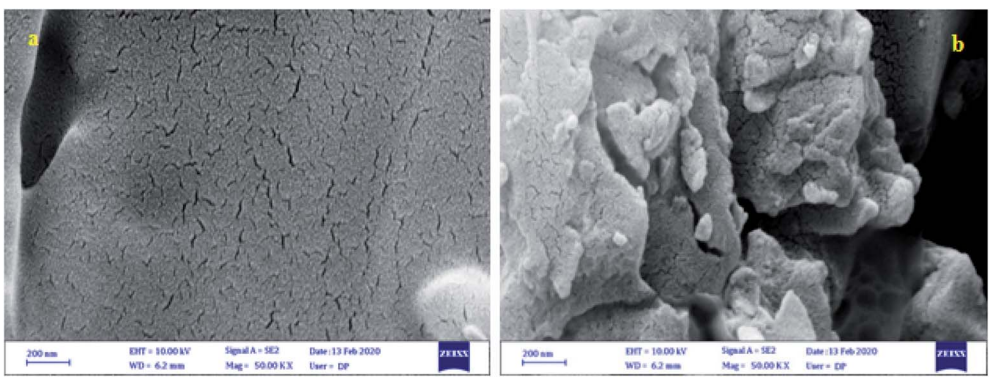

Fig. 6 Scanning electron microscopy (SEM) images of CQDs–NH_2 (a) and CQDs–$N(CH_2PO_3H_2)_2$ (b).

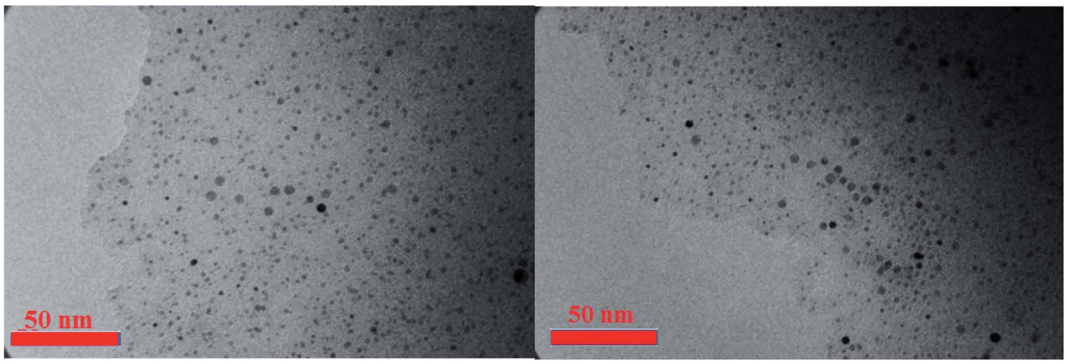

Fig. 7 Transmission electron microcopy (TEM) images of CQDs–$N(CH_2PO_3H_2)_2$.

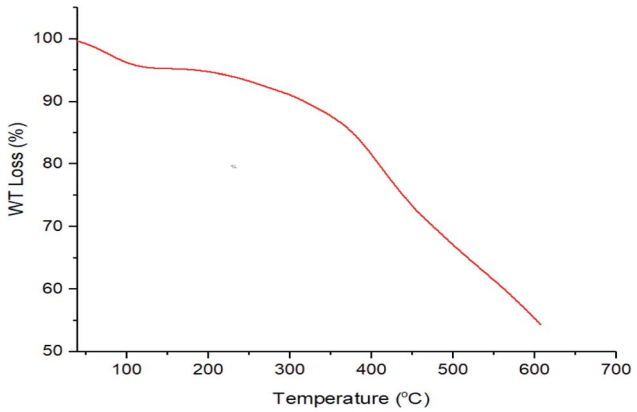

Fig. 8 Thermal gravimetric (TG) analysis of CQDs–$N(CH_2PO_3H_2)_2$.

reaction of 4-chloro-benzaldehyde (1 mmol, 0.14 g), 3-(1*H*-indol-3-yl)-3-oxopropanenitrile (1 mmol, 0.184 g) and malononitrile (1.1 mmol, 0.073 g) as a model for the optimization of the reaction conditions. The optimization data is listed in Table 1. As shown in Table 1, the best synthesis of 2-amino-4-(4-chlorophenyl)-6-(1*H*-indol-3-yl)-4*H*-pyran-3,5-dicarbonitrile was achieved in the presence of 10 mg CQDs–$N(CH_2PO_3H_2)_2$ in EtOH (5 mL) as the solvent (entry 1, Table 1). The model reaction was also studied using several solvents such as H_2O, CH_3CN, *n*-hexane, $CHCl_3$, toluene, MeOH, DMF, EtOH, CH_2Cl_2 and EtOAc (5 mL), as well as a solvent-free condition, in the presence of 10 mg of CQDs–$N(CH_2PO_3H_2)_2$. The results of the reaction show that the yield and time were not improved when using other amounts of catalyst (Table 1, entries 16–18).

Table 1 Effects of different amounts of catalyst, temperature and solvent (5 mL) on the synthesis of 2-amino-4-(4-chlorophenyl)-6-(1*H*-indol-3-yl)-4*H*-pyran-3,5-dicarbonitrile

Entry	Solvent	Catalyst (mg)	Temp. (°C)	Time (min)	Yield (%)
1	EtOH	10	Reflux	25	89
2	EtOH	10	50	45	55
3	EtOH	10	25	80	30
4	EtOH	5	Reflux	35	70
5	EtOH	20	Reflux	30	75
6	EtOH	—	Reflux	120	25
7	DMF	10	100	90	60
8	H_2O	10	Reflux	120	—
9	CH_3CN	10	Reflux	120	Trace
10	*n*-hexane	10	Reflux	120	—
11	$CHCl_3$	10	Reflux	100	50
12	Toluene	10	Reflux	120	—
13	MeOH	10	Reflux	50	60
14	CH_2Cl_2	10	Reflux	50	35
15	EtOAc	10	Reflux	120	—
16	—	10	100	30	60
17	—	10	25	120	35
18	—	10	50	50	45

After optimizing the reaction conditions, CQDs–$N(CH_2PO_3H_2)_2$(10 mg) was applied to synthesise a good range of desired compounds using various aromatic aldehydes bearing electron-donating groups, electron-withdrawing groups and heterocycles, as well as malononitrile and 3-(1*H*-indol-3-yl)-3-oxopropanenitrile derivatives, both in refluxing EtOH or ultrasonic irradiation conditions (methods A and B, respectively). As shown in Table 2 the obtained results indicated that CQDs–$N(CH_2PO_3H_2)_2$ is appropriate for the preparation of target molecules in high to excellent yields with short reaction times (methods A and B).

In the proposed mechanism, the aldehyde is activated with a proton of the acidic functional groups of CQDs–$N(CH_2PO_3H_2)_2$ and intermediate (**I**) is prepared by the reaction of malononitrile with the loss of one molecule of H_2O. In the second step, 3-(1*H*-indol-3-yl)-3-oxopropanenitrile reacts with intermediate (**I**) to give intermediate (**II**) after tautomerization. Then, intermediate (**II**) gives the desired product after intramolecular cyclization and the loss of another molecule of H_2O (Scheme 3).

To compare the efficiency of the described CQDs–$N(CH_2PO_3H_2)_2$ for the synthesis of 2-amino-6-(2-methyl-1*H*-indol-3-yl)-4-phenyl-4*H*-pyran-3,5-dicarbonitrile that was achieved in the presence of 10 mg of the catalyst by the reaction of 4-chloro-benzaldehyde (1 mmol, 0.14 g), 3-(1*H*-indol-3-yl)-3-oxopropanenitrile (1 mmol, 0.184 g) and malononitrile (1.1 mmol, 0.073 g) under the above-mentioned optimized reaction conditions, various organic and inorganic solid acid catalysts for the above reaction were tested (Table 3). As Table 3 indicates, CQDs–$N(CH_2PO_3H_2)_2$ is the best choice for the synthesis of 2-amino-6-(2-methyl-1*H*-

Table 2 Synthesis of 2-amino-4-(4-chlorophenyl)-6-(1*H*-indol-3-yl)-4*H*-pyran-3,5-dicarbonitrile derivatives using CQDs–$N(CH_2PO_3H_2)_2$ under refluxing EtOH (method A) and ultrasonic irradiation (method B)

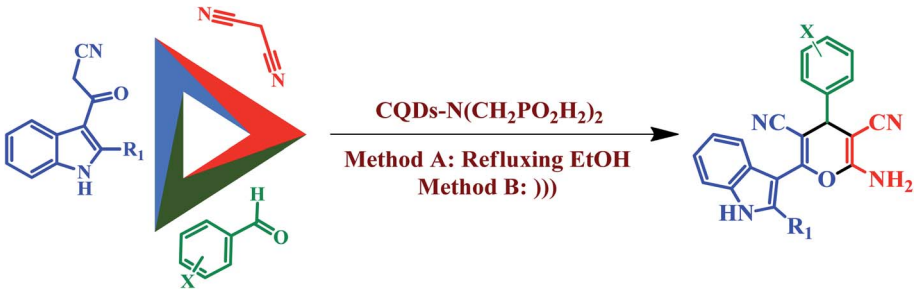

				Method A		Method B		
Entry	R_1	X	Product	Time (min)	Yield (%)	Time (min)	Yield (%)	MP (°C)
L1	Me	4-OMe	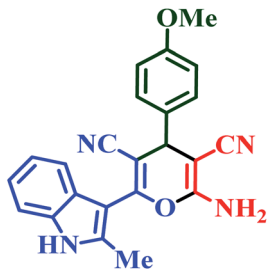	25	87	6	93	263–265
L2	Me	4-Cl	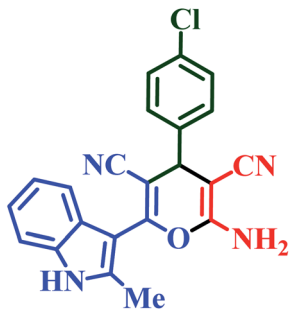	25	89	10	94	268–270
L3	Me	2-Cl	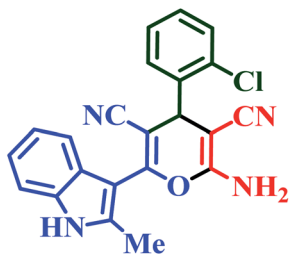	20	88	10	92	236–238
L4	Me	4-NO_2	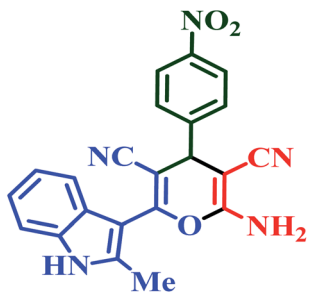	10	90	Immediate	95	284–286 (ref. 46)

Table 2 (*Contd.*)

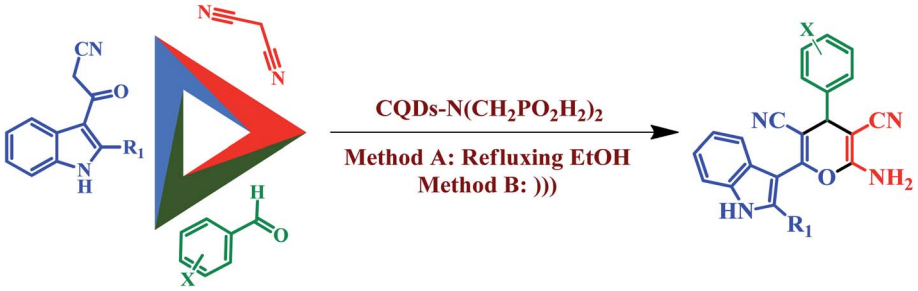

Entry	R_1	X	Product	Method A Time (min)	Method A Yield (%)	Method B Time (min)	Method B Yield (%)	MP (°C)
L5	Me	3-NO_2	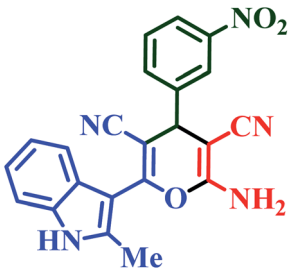	10	90	Immediate	95	252–254 (ref. 46)
L6	Me	4-Br	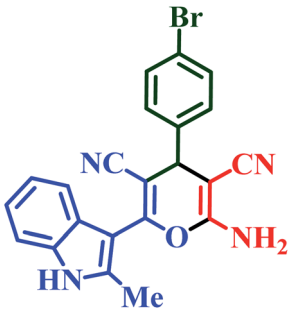	20	88	7	92	267–269 (ref. 46)
L7	Me	3,4-OMe	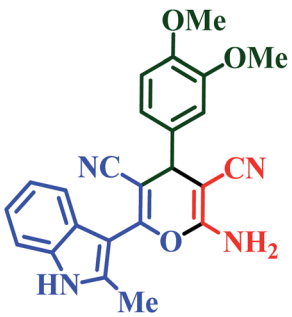	20	85	8	91	205–207
L8	Me	4-Py	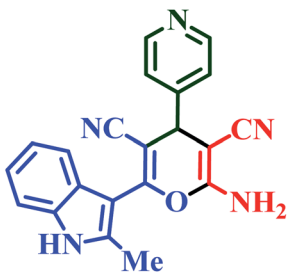	10	85	Immediate	93	226–228

Table 2 (*Contd.*)

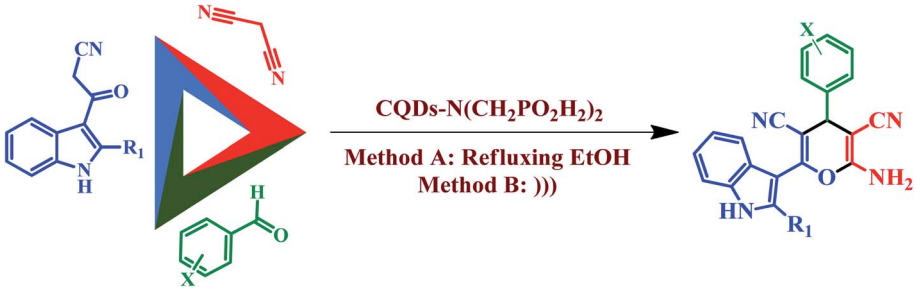

Entry	R_1	X	Product	Method A Time (min)	Method A Yield (%)	Method B Time (min)	Method B Yield (%)	MP (°C)
L9	Me	4-CN	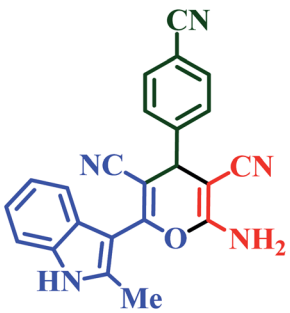	30	87	8	92	257–259
L10	Me	3-Py	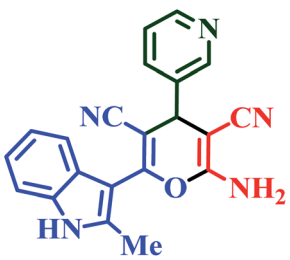	10	87	Immediate	95	220–222
I1	H	4-Cl	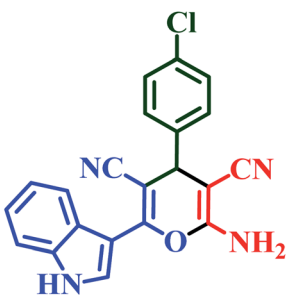	23	85	8	92	254–256 (ref. 46)
I2	H	4-Br	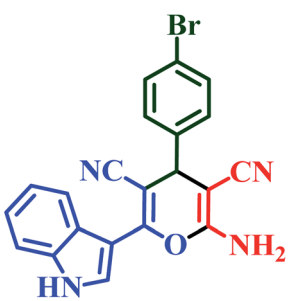	20	86	7	93	210–212 (ref. 44)

Table 2 (*Contd.*)

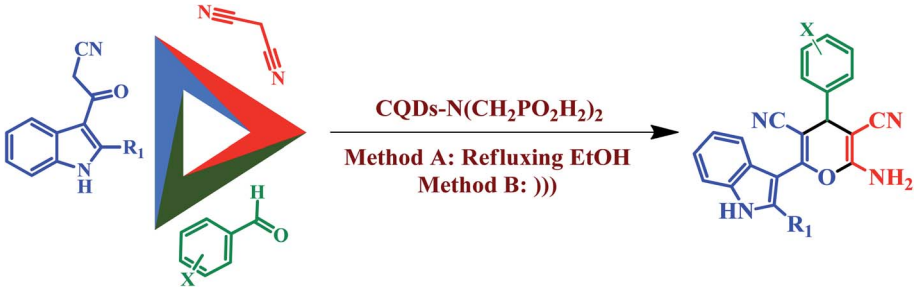

Entry	R_1	X	Product	Method A Time (min)	Method A Yield (%)	Method B Time (min)	Method B Yield (%)	MP (°C)
I3	H	3-NO_2	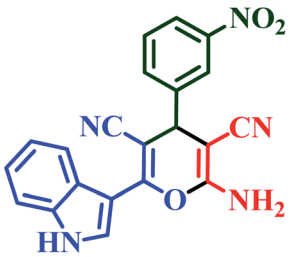	10	88	Immediate	95	248–250 (ref. 45)
I4	H	4-NO_2	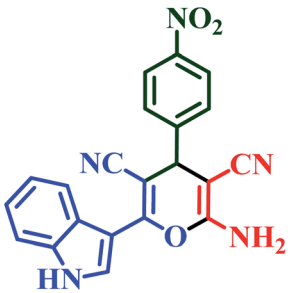	10	88	Immediate	94	239–241 (ref. 44)
I5	H	2-Naph	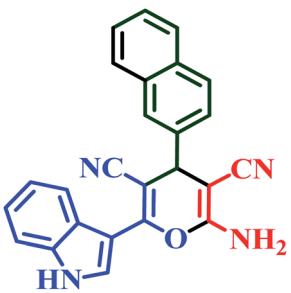	27	80	13	87	205–207 (ref. 45)
I6	H	4-Py	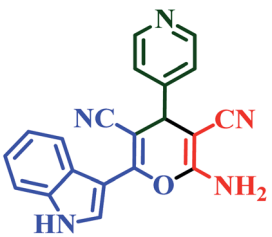	10	87	Immediate	94	220–222

Table 2 (*Contd.*)

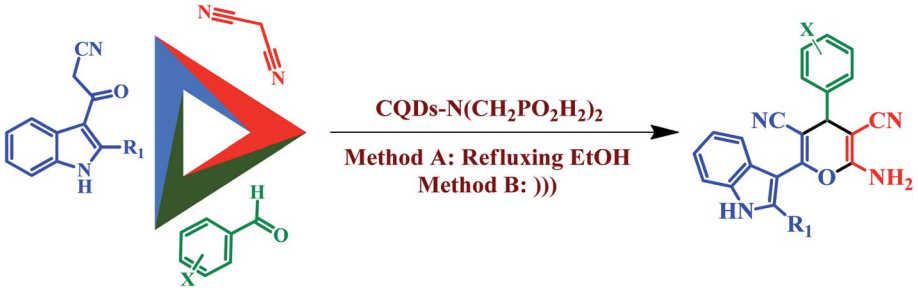

Entry	R_1	X	Product	Method A Time (min)	Method A Yield (%)	Method B Time (min)	Method B Yield (%)	MP (°C)
I7	H	4-OMe	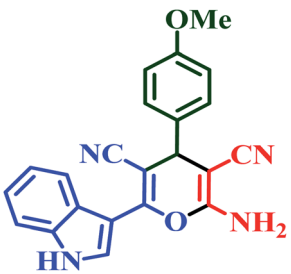	20	80	7	94	246–248 (ref. 45)
I8	H	4-CN	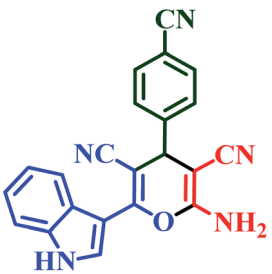	15	82	6	93	260–262
I9	H	2,6-Cl	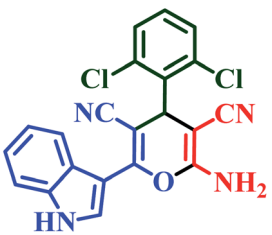	30	65	15	75	238–240
I10	H	3-Py	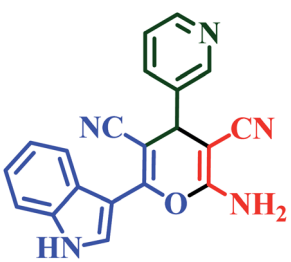	10	85	Immediate	95	238–240
I11	H	3,4-OMe	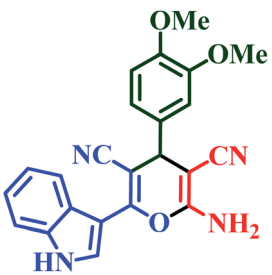	20	85	7	90	228–230 (ref. 45)

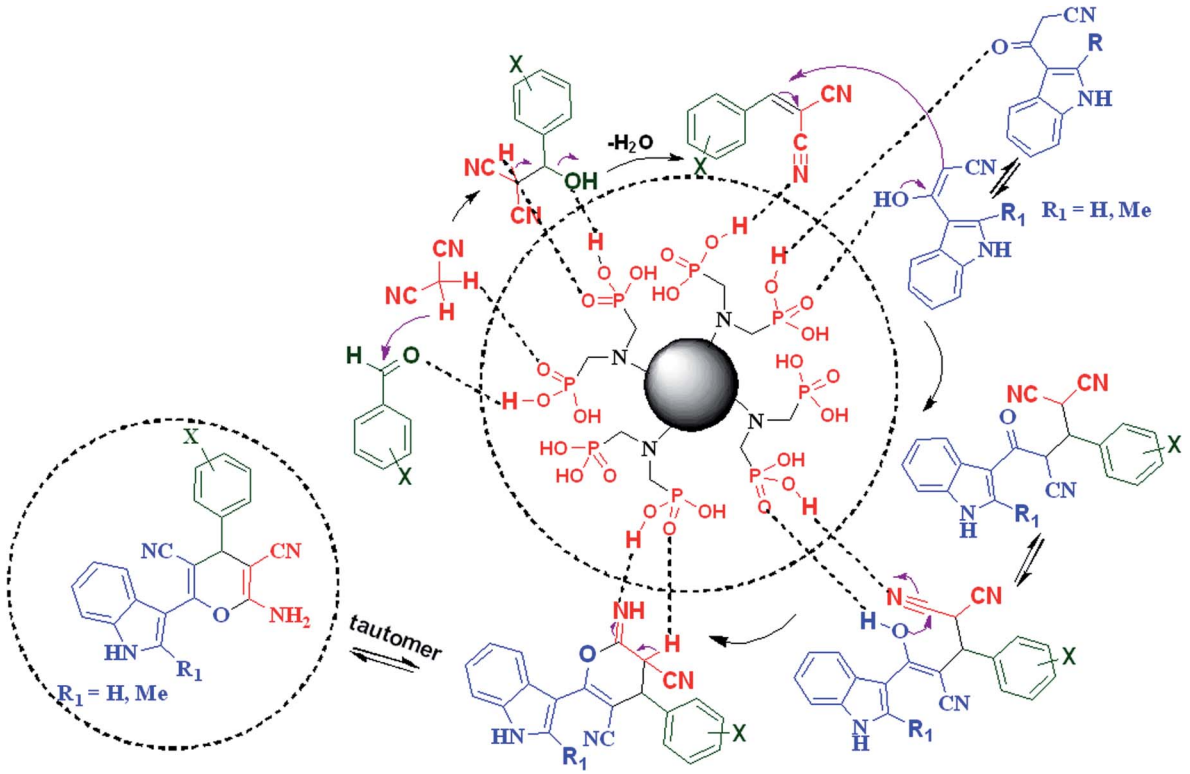

Scheme 3 Proposed mechanism for the synthesis of 2-amino-4-(4-chlorophenyl)-6-(1*H*-indol-3-yl)-4*H*-pyran-3,5-dicarbonitrile.

Table 3 Synthesis of 2-amino-4-(4-chlorophenyl)-6-(1*H*-indol-3-yl)-4*H*-pyran-3,5-dicarbonitrile the presence of various catalysts using method A

Entry	Catalyst	(mol %)	Time (min)	Yield (%)
1	$FeCl_3$	10	80	25
2	H_2SO_4	10	120	20
3	Fe_3O_4	10 mg	120	Trace
4	NH_4NO_3	10	90	25
5	CF_3SO_3H	10	70	35
6	GTBSA[47]	10	120	15
7	MIL-100(Cr)/NHEtN $(CH_2PO_3H_2)_2$ (ref. 21)	10	80	60
8	$H_3[p(W_3O_{10})_4]\cdot XH_2O$	10	120	Trace
9	SBA-15/$(CH_2)_3N(CH_2PO_3H_2)$ $(CH_2)_2$–$N(CH_2PO_3H_2)_2$ (ref. 17*b*)	10	90	62
10	[PVI-SO_3H]$FeCl_4$ (ref. 48)	10	100	48
11	*p*-TSA	10	120	48
12	SSA[49]	10 mg	110	50
13	Et_3N	10	120	—
14	MHMHPA[18]	10	90	50
15	Nano-SB-[PSIM]Cl[50]	—	—	—
16	[Py-SO_3H]Cl[51]	10	120	35
17	APVPB[52]	10 mg	80	60
18	Fe_3O_4@Co(BDC)-NH_2 (ref. 53)	10 mg	70	65
19	H_3PO_3	10	60	63
20	CQDs	10 mg	45	70
21	CQDs-N$(CH_2PO_3H_2)_2$ (this work)	10 mg	25	89

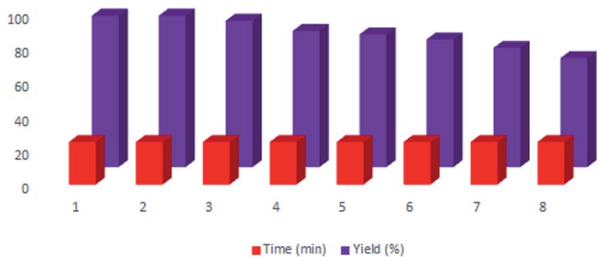

Fig. 9 Recyclability of CQDs–N$(CH_2PO_3H_2)_2$ for the synthesis of 4*H*-pyran-3,5-dicarbonitrile derivatives.

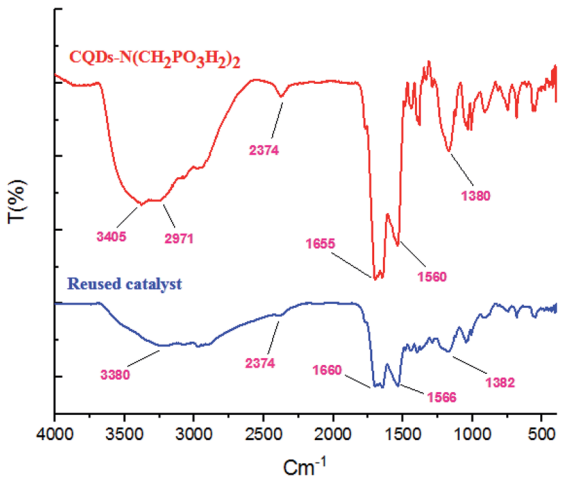

Fig. 10 The characterization of the reused catalysts after seven runs using FT-IR spectroscopy.

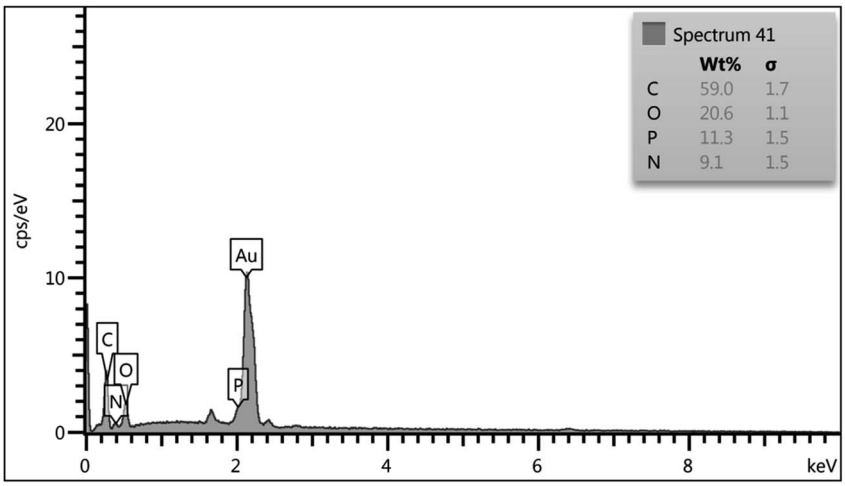

Fig. 11 The characterization of the reused catalysts after seven runs using energy dispersive X-ray analysis (EDX).

indol-3-yl)-4-phenyl-4*H*-pyran-3,5-dicarbonitrile derivatives; due to the shorter reaction times, higher yields and amount of applied catalyst. Also, the reusability of CQDs–$N(CH_2PO_3H_2)_2$ as a catalyst for the preparation of 2-amino-6-(2-methyl-1*H*-indol-3-yl)-4-phenyl-4*H*-pyran-3,5-dicarbonitrile derivatives was examined in the above reaction. The results show that the catalyst has the potential to be recycled and reused up to 7 times without a significant decrease in its catalytic activity (Fig. 9).CQDs–$N(CH_2PO_3H_2)_2$ was also characterized by FT-IR and energy dispersive X-ray analysis (EDX) analysis after its application in the reaction. These spectra were same as those of the fresh catalyst (Fig. 10 and 11).

4. Conclusion

In conclusion, we have designed and introduced CQDs–$N(CH_2PO_3H_2)_2$ as a novel heterogeneous nano-catalyst. It was identified using various techniques. CQDs–$N(CH_2PO_3H_2)_2$, as an efficient catalyst, was applied for the synthesis of multi substituted 4*H*-pyran-3,5-dicarbonitrile with indole moieties as candidates with biological interest. The presented methodology is not suitable for synthesis of pyridines with indole moieties. A short reaction time, clean and mild reaction conditions and the recycling of the catalyst are the major advantages of the presented work.

Conflicts of interest

There are no conflicts to declare.

Acknowledgements

We thank the Bu-Ali Sina University and Iran National Science Foundation (INSF) (grant number: 98020070) for financial support.

References

1 M. J. Molaei, *Anal. Methods*, 2020, **12**, 1266.
2 M. J. Molaei, *Sol. Energy*, 2020, **196**, 549.
3 X. Kou, S. Jiang, S. J. Park and L. Y. Meng, *Dalton Trans.*, 2020, **49**, 6915–6928.
4 J. M. Katzen, C. Tserkezis, Q. Cai, L. H. Li, J. M. Kim, G. Lee, G. Yi, W. R. Hendren, E. J. G. Santos, R. M. Bowman and F. Huang, *ACS Appl. Mater. Interfaces*, 2020, **12**, 19866.
5 G. Kalaiyarasan, J. Joseph and P. Kumar, *ACS Omega*, 2020, **5**, 22278.
6 F. Li, T. Li, C. Sun, J. Xia, Y. Jiao and H. Xu, *Angew. Chem., Int. Ed.*, 2017, **56**, 9910.
7 X. Xu, R. Ray, Y. Gu, H. J. Ploehn, L. Gearheart, K. Raker and W. A. Scrivens, *J. Am. Chem. Soc.*, 2004, **126**, 12736.
8 H. Li, X. He, Z. Kang, H. Huang, Y. Liu, J. Liu, S. Lian, C. H. A. Tsang, X. Yang and S. T. Lee, *Angew. Chem.*, 2010, **122**, 4532.
9 W. Su, R. Guo, F. Yuan, Y. Li, X. Li, Y. Zhang, S. Zhou and L. Fan, *J. Phys. Chem. Lett.*, 2020, **11**, 1357.
10 B. C. Martindale, G. A. Hutton, C. A. Caputo and E. Reisner, *J. Am. Chem. Soc.*, 2015, **137**, 6018.
11 B. B. Karakoçak, A. Laradji, T. Primeau, M. Y. Berezin, S. Li and N. Revi, *ACS Appl. Mater. Interfaces*, 2021, **13**, 277.
12 K. M. Chan, W. Xu, H. Kwon, A. M. Kietrys and E. T. Kool, *J. Am. Chem. Soc.*, 2017, **139**, 13147.
13 X. Xiao, Z. Shao and L. Yu, *Chin. Chem. Lett.*, 2021, **23**, 4647.
14 X. Wang, Y. Feng, P. Dong and J. Huang, *Front. Chem.*, 2019, **7**, 671.
15 (*a*) C. Fujun, Y. Ping, L. Xiguang, L. Chunping and Q. Rongjun, *Renewable Energy*, 2014, **71**, 61; (*b*) M. F. Mady and M. A. Kelland, *Energy Fuels*, 2017, **31**, 4603; (*c*) A. Kadous, M. Didi and D. Villemin, *J. Radioanal. Nucl. Chem.*, 2010, **284**, 431.
16 S. Moradi, M. A. Zolfigol, M. Zarei, D. A. Alonso and A. Khoshnood, *ChemistrySelect*, 2018, **3**, 3042.
17 (*a*) M. Zarei, M. A. Zolfigol, A. R. Moosavi-Zare, E. Noroozizadeh and S. Rostamnia, *ChemistrySelect*, 2018,

3, 12144; (*b*) F. Jalili, M. Zarei, M. A. Zolfigol, S. Rostamnia and A. R. Moosavi-Zare, *Microporous Mesoporous Mater.*, 2020, **294**, 109865.

18 J. Afsar, M. A. Zolfigol, A. Khazaei, M. Zarei, Y. Gu, D. A. Alonso and A. Khoshnood, *Mol. Catal.*, 2020, **482**, 110666.

19 S. Babaee, M. Zarei, H. Sepehrmansourie, M. A. Zolfigol and S. Rostamnia, *ACS Omega*, 2020, **5**, 6240.

20 S. Babaee, M. Zarei, M. A. Zolfigol, S. Khazalpour, M. Hasani, U. Rinner, R. Schirhagl, N. Norouzi and S. Rostamnia, *RSC Adv.*, 2021, **11**, 2141.

21 H. Sepehrmansouri, M. Zarei, M. A. Zolfigol, A. R. Moosavi-Zare, S. Rostamnia and S. Moradi, *Mol. Catal.*, 2020, **481**, 110303.

22 S. Kalhor, M. Zarei, H. Sepehrmansourie, M. A. Zolfigol, H. Shi, J. Wang, J. Arjomandi, M. Hasanie and R. Schirhagl, *Mol. Catal.*, 2021, **507**, 111549.

23 (*a*) A. Varvaresou, A. Tsantili-Kakoulidou, T. Siatra-Papastaikoudi and E. Tiligada, *Arzneimittelforschung*, 2000, **50**, 48; (*b*) J. Slaett, I. Romero and J. Bergman, *Synth.*, 2004, **16**, 2760; (*c*) F. Palluotto, A. Carotti, G. Casini, M. Ferappi, A. Rosato, C. Vitali and F. Campagna, *Il Farmaco*, 1999, **54**, 191; (*d*) M. Shiri, *Chem. Rev.*, 2012, **112**, 3508; (*e*) M. Shiri, M. A. Zolfigol, H. G. Kruger and Z. Tanbakouchian, *Chem. Rev.*, 2010, **110**, 2250.

24 (*a*) P. Kutsky, T. M. Dzurilla and A. Sabova, *Collect. Czech. Chem. Commun.*, 1999, **64**, 348; (*b*) P. Kutschy, M. Dzurilla, M. Takasugi, M. Török, I. Achbergerová, R. Homzová and M. Rácová, *Tetrahedron*, 1998, **54**, 3549.

25 S. A. Zotova, T. M. Korneeva, V. I. Shvedov, N. I. Fadeeva, I. A. Leneva, I. T. Fedyakina, M. L. Khristova, I. S. Nikolaeva, V. V. Peters and T. A. Gus'kova, *Pharm. Chem. J.*, 1995, **29**, 57.

26 N. V. Lakshmi, P. Thirumurugan, K. M. Noorulla and P. T. Perumal, *Bioorg. Med. Chem. Lett.*, 2010, **20**, 5054.

27 R. D. Dillard, N. J. Bach, S. E. Draheim, D. R. Berry, D. G. Carlson, N. Y. Chirgadze and J. P. Wery, *J. Med. Chem.*, 1996, **39**, 5119.

28 S. M. Gomha and H. A. Abdel-Aziz, *Bull. Korean Chem. Soc.*, 2012, **33**, 2985.

29 S. Battagba, E. Boldrini, F. D. Settimo, G. Dondio, C. L. Motta, A. M. Marini and G. Primofiore, *Eur. J. Med. Chem.*, 1999, **34**, 93.

30 L. Garuti, M. Roberti, T. Rossi, M. Castelli and M. Malagoli, *Eur. J. Med. Chem.*, 1998, **33**, 43.

31 (*a*) M. A. Radwan, E. A. Ragab, N. M. Sabry and S. M. El-Shenawy, *Bioorg. Med. Chem.*, 2007, **15**, 3832; (*b*) S. L. Zhu, S. J. Ji, X. M. Su, C. Sun and Y. Liu, *Tetrahedron Lett.*, 2008, **49**, 1777; (*c*) A. A. Fadda, A. El-Mekabaty, I. A. Mousa and K. M. Elattar, *Synth. Commun.*, 2014, **44**, 1579; (*d*) P. Thirumurugan, A. Nandakumar, D. Muralidharan and P. T. Paramasivan, *J. Comb. Chem.*, 2010, **12**, 161.

32 D. Kumar, P. Sharma, H. Singh, K. Nepali, G. K. Gupta, S. K. Jain and F. Ntie-Kang, *RSC Adv.*, 2017, **7**, 36977.

33 Saigal, M. Irfan, P. Khan, M. Abid and M. M. Khan, *ACS Omega*, 2019, **4**, 16794.

34 P. K. Singh and O. Silakari, *ChemMedChem*, 2018, **13**, 1071.

35 S. Gupta, S. Adhikary, R. K. Modukuri, D. Choudhary, R. Trivedi and K. V. Sashidhara, *Bioorg. Med. Chem. Lett.*, 2018, **28**, 1719.

36 S. P. Khare, T. R. Deshmukh, S. V. Akolkar, J. N. Sangshetti, V. M. Khedkar and B. B. Shingate, *Res. Chem. Intermed.*, 2019, **45**, 5159.

37 Z. Tashrifi, M. Mohammadi-Khanaposhtani, H. Hamedifar, B. Larijani, S. Ansari and M. Mahdavi, *Mol. Diversity*, 2020, 1.

38 (*a*) P. N. Amaniampong and F. Jerome, *Curr. Opin. Green Sustain. Chem.*, 2020, **22**, 7; (*b*) J. Amaro-Gahete, R. Klee, D. Esquivel, J. R. Ruiz, C. Jiménez-Sanchidrián and F. J. Romero-Salguero, *Ultrason. Sonochem.*, 2019, **50**, 59.

39 F. Bigdeli, F. Rouhani, A. Morsali and A. Ramazani, *Ultrason. Sonochem.*, 2020, **62**, 104862.

40 J. Schneider, C. J. Reckmeier, Y. Xiong, M. von Seckendorff, A. S. Susha, P. Kasák and A. L. Rogach, *J. Phys. Chem. C*, 2017, **121**, 2014.

41 M. Shiri, *Chem. Rev.*, 2012, **112**, 3508.

42 M. Shiri, M. A. Zolfigol, H. G. Kruger and Z. Tanbakouchian, *Chem. Rev.*, 2010, **110**, 2250.

43 H. Kooshki, A. Sobhani-Nasab, M. Eghbali-Arani, F. Ahmadi, V. Ameri and M. Rahimi-Nasrabadi, *Sep. Purif. Technol.*, 2019, **211**, 873.

44 T. Chen, X. P. Xu and S. J. Ji, *J. Heterocycl. Chem.*, 2013, **50**, 244.

45 N. V. Lakshmi, P. Thirumurugan, K. M. Noorulla and P. T. Perumal, *Bioorg. Med. Chem. Lett.*, 2010, **20**, 5054.

46 L. Kheirkhah, M. Mamaghani, A. Yahyazadeh and N. O. Mahmoodi, *Appl. Organomet. Chem.*, 2018, **32**, 4072.

47 M. Zarei, H. Sepehrmansourie, M. A. Zolfigol, R. Karamian and S. H. Moazzami Farida, *New J. Chem.*, 2018, **42**, 14308.

48 H. Sepehrmansourie, M. Zarei, R. Taghavi and M. A. Zolfigol, *ACS Omega*, 2019, **4**, 17379.

49 (*a*) M. A. Zolfigol, *Tetrahedron*, 2001, **57**, 9509; (*b*) H. Sepehrmansourie, *Iran. J. Catal.*, 2020, **10**, 175.

50 A. Zare, M. Merajoddin, A. R. Moosavi-Zare, M. Zarei, M. H. Beyzavi and M. A. Zolfigol, *Res. Chem. Intermed.*, 2016, **42**, 2365.

51 A. R. Moosavi-Zare, M. A. Zolfigol, M. Zarei, V. Khakyzadeh and A. Hasaninejad, *Appl. Catal., A*, 2013, **467**, 61.

52 E. Noroozizadeh, A. R. Moosavi-Zare, M. A. Zolfigol, M. Zarei, R. Karamian, M. Asadbegy, S. Yari and S. H. M. Farida, *J. Iran. Chem. Soc.*, 2018, **15**, 471.

53 H. Sepehrmansourie, M. Zarei, M. A. Zolfigol, S. Babaee and S. Rostamnia, *Sci. Rep.*, 2021, **11**, 5279.